Emergent Materials (2022) 5:519–528
https://doi.org/10.1007/s42247-021-00167-9

ORIGINAL ARTICLE

Effects of chitosan-glycerol phosphate hydrogel on the maintenance and homing of hAd-MSCs after xenotransplantation into the rat liver

Aliakbar Haddad-Mashadrizeh[1] · Maryam M. Matin[2,3] · Fahimeh Shahabipour[4,5] · Shabnam Ensandost[1] · Alireza Zomorodipour[6] · Ahmad Reza Bahrami[1,2]

Received: 12 December 2020 / Accepted: 19 January 2021 / Published online: 4 March 2021

Abstract

Problems associated with the treatment of liver failure necessitate more research on advanced strategies like cell-based therapy and tissue engineering. Since cell therapy approaches suffer from some limitations, tissue engineering and material science converge the sight onto stem cell-biomaterial based therapy. In this study, the human adipose-derived mesenchymal stem cells (hAd-MSCs), carrying ectopic fluorescent reporter genes, were encapsulated in the chitosan-β-glycerol phosphate hydroxyethyl cellulose (β-GP-HEC) and transplanted into the right lobe of the intact liver of Wistar rats (as cell-laden scaffolds). In addition, labeled hAd-MSCs were injected into the liver (as scaffold-free groups). All experimental groups were monitored after 15, 45, 90, and 180 days of transplantation. Fluorescence microscopy and histological evaluations were used to monitor the migration and distribution of cells within the two test groups along with their related controls, during the 6-month follow-up. Moreover, the ability of cells to migrate to other tissues was detected by quantitative PCR. Macroscopic inspection during this period showed no evidence of pathological inflammatory responses. Microscopic observations revealed that the injected cells were detectable at the target organ, for at least 6 months in both scaffold and scaffold-free groups. However, the scaffold-free samples showed signs of reduction in cellular augmentation over time. The molecular assessment also confirmed that the application of scaffold in vivo reduced unnecessary cell migration into other organs. In conclusion, the application of cell-seeded β-GP-HEC scaffold not only improved cell survival but also reduced the rate of cellular escape from the target area of transplantation.

Keywords Cell therapy · hAd-MSCs · Reporter genes · Scaffold · Chitosan-glycerol phosphate hydrogel

1 Introduction

Liver abnormalities induced by autoimmune hepatitis, alcohol abuse, non-alcoholic fatty liver disease, and metabolic disorders lead to end-stage liver failure and liver cancer, which account for progressive causes of death worldwide [1, 2]. Liver transplantation has been considered as an established treatment for end-stage liver diseases. However, this approach is limited by the scarcity of liver donors leading to numerous deaths while patients are on a waiting list [1, 2]. Multiple other therapies have been applied to treat patients with end-stage liver diseases by enhancing liver regeneration [3]. Besides liver transplantation, hepatocyte transplantation is a useful strategy to accelerate liver regeneration [2]. Liver transplantation requires a surgery with the inherent risks of related complications. However, hepatocyte transplantation has some advantages in terms of providing less invasive and less expensive procedures compared with liver transplantation. On the other hand, these cells have displayed less

✉ Ahmad Reza Bahrami
AR-Bahrami@um.ac.ir

Maryam M. Matin
matin@um.ac.ir

1 Industrial Biotechnology Research Group, Institute of Biotechnology, Ferdowsi University of Mashhad, Mashhad, Iran

2 Department of Biology, Faculty of Science, Ferdowsi University of Mashhad, Mashhad, Iran

3 Novel Diagnostics and Therapeutics Research Group, Institute of Biotechnology, Ferdowsi University of Mashhad, Mashhad, Iran

4 National Cell Bank of Iran, Pasteur Institute of Iran, Tehran, Iran

5 Skin Research Center, Shahid Beheshti University of Medical Science, Tehran, Iran

6 National Institute of Genetic Engineering and Biotechnology, Tehran, Iran

functional activity in vitro, which has limited their therapeutic applications [4]. It was indicated that only a small percentage of primary hepatocytes migrate into host liver tissue, resulting in weak therapeutic effects in vivo [5]. According to clinical studies, cell therapy with mesenchymal stem cells has emerged as an alternative strategy to hepatocyte transplantation for enhancing liver regeneration [6].

Mesenchymal stem cells represent a promising source for regenerative medicine. These cells can be derived from various tissues, including bone marrow [7], umbilical cord blood [8], placenta [9], scalp tissue [10], amniotic fluid [11], and adipose tissue [12]. In particular, adipose tissue-derived mesenchymal stem cells are recognized as a readily available adult multipotent stem cell source with an obvious hepatogenic capability in vitro and in vivo [13]. Transplantation of multipotent hAd-MSCs has drawn widespread attention as a regenerative therapy tool in clinical applications, mainly due to convenient large-scale harvest from subcutaneous fat, relieving inflammation, wound healing, and differentiation potential into multiple lineages, including adipocytes, chondrocytes, osteocytes, neurons, and hepatocytes. Thus, hAd-MSCs have been suggested as an alternative cell source in cell-based therapy to heal the hepatic injury [14]. Previous studies have successfully used Ad-MSCs for cell therapy of liver fibrosis in animal models owing to the efficient production of fibrinolytic enzyme and cytokines [15]. Despite unique characteristics, the safety and the mechanism of action are major issues that need to be elucidated. Thus, both cell fate determination and homing in vivo have paramount importance after transplantation succeeds in the clinical translation of stem cell therapy [16]. In addition, the effective local transplantation of Ad-MSCs to the target organs and their subsequent proliferation are other challenges remaining to be resolved [17]. Thus, some lines of research have focused on how to improve the number of residing transplanted cells in the liver. Following robust developments in access to the cell sources, the field of cell therapy is still suffering from setbacks such as cell delivery and maintenance. Reports have revealed that using conventional methods to transplant Ad-MSCs into the liver by splenic injection is followed by a big loss of planted cells [18]. Researchers are trying to develop suitable biomaterials, to be used for cellular encapsulation, in order to improve the efficiency of cell therapy [17]. Some studies have been conducted to design engineered constructs to overcome these shortcomings and fabricate equivalent functional hepatocytes in vitro [19, 20].

In tissue engineering, fabricating scaffolds that maintain cellular function and viability after implantation in the body has been suggested as a critical issue [21]. In this context, some studies have indicated that both synthetic and natural three-dimensional (3D) scaffolds could provide an environment, which supports the maintenance and growth of hepatocytes. However, the selection of suitable biomaterials or synthetic matrices for hepatic tissue engineering remains a problem [22].

Chitosan is a linear polysaccharide, which has been broadly applied in tissue engineering, including wound healing, and drug delivery vehicles [23–26] (Prudden, Migel et al. 1970, Muzzarelli, Baldassarre et al. 1988, VandeVord, Matthew et al. 2002, Hoemann, Chenite et al. 2007). Although chitosan is known for its excellent biocompatibility, it has poor solubility in physiological conditions. In this regard, the application of disodium glycerol phosphate (GP) can maintain chitosan solubility at neutral pH, resulting in thermogelling at body temperature [27]. In addition, chitosan-GP solution combined with a hydroxyethyl cellulose (HEC) embedded cell suspension, has successfully been applied for chondral defects in rabbits [28]. In this study, we aimed to investigate and compare the fate of hAd-MSCs in two representing groups; injected cells as a scaffold-free group and encapsulated in the CH-β-GP-HEC scaffold, which were transplanted in the rat liver, for up to 6 months. For monitoring the cells in vivo, hAd-MSCs were labeled with green and red fluorescent protein reporter genes. The effects of glycerol phosphate hydrogel on retaining, survival, and migration of the cells were assessed using immunofluorescence assay, histological staining, and qPCR.

2 Materials and methods

2.1 Isolation and culture of human adipose-derived mesenchymal stem cells

Human Ad-MSCs were derived from liposuction waste tissue by means of collagenase digestion and differential centrifugation [29]. After treatment with equal volumes of phosphate-buffered saline (PBS) containing 100 units/ml penicillin and 100 μg/ml streptomycin antibiotics, the adipose tissue was transferred into 0.1% collagenase type 1 (Sigma) in Hanks' balanced salt solution, and incubated for 1 h at 37 °C under agitation. The collagenase was then inactivated with diluted Dulbecco's modified Eagle's medium with high glucose (DMEM-HG) (Gibco), supplemented with 10% (v/v) fetal bovine serum (FBS) (Gibco). The suspension was then centrifuged at 800*g* for 5 min. The resulting pellet was resuspended in DMEM-HG (containing 10% FBS) and transferred into the tissue culture plates (Nunc) at 1000–3500 cells/cm^2. Cultures were washed with PBS, 24–48 h after plating, to remove the unattached cells, fed with fresh medium, and maintained at 37 °C with 5% CO_2. When they reached about 70% confluence, cells were trypsinized (0.25%; Invitrogen) and plated at a density of 5000 cells/cm^2. Cultures were passaged repeatedly after confluence until passage 3.

2.1.1 Human Ad-MSC transduction with pLEX-JRed/TurboGFP

Human Ad-MSCs were genetically modified by exposure to the pLEX-JRed/TurboGFP using the lentiviral transduction system. Lentiviral particles were produced by transfection of HEK-293T cells with three plasmids: pLEX-JRed/TurboGFP (21 μg) (Open Biosystems), packaging vector psPAX2 (21 μg), and envelope plasmid pMD.2G (10.5 μg) (Trono Lab). Culture media containing the virus particles were harvested 24, 48, and 72 h post-transfection, and centrifuged for 5 min at 500*g* (4 °C) to pellet the detached cells, and their debris were filtered through a 0.45 μm filter. Subsequently, the virus was quantified using a p24 ELISA kit (DIA.PRO, Italy) to detect the HIV-p24 core protein of the vector. For viral transduction of the cells, the undifferentiated hAd-MSCs at passage 3, were seeded at a concentration of 3×10^6 cells per flask (T75) and maintained in a humidified incubator at 37 °C and 5% CO_2. After proper cellular attachment, they were subjected to 10 ml of the viral supernatant. The efficiency of the transduction was determined according to the GFP expression using fluorescent microscopy. At 72 h of virus infection, the culture was treated with puromycin (1 μg/ml) for selection (Sigma-Aldrich). After purification of the labeled hAd-MSCs, osteogenic and adipogenic differentiation assays were performed to verify the identity of the labeled hAd-MSCs.

2.1.2 Osteogenic and adipogenic differentiation of hAd-MSCs in vitro

Human Ad-MSCs, before and after lentivirus transduction, were cultured in 6-well plates at 100,000 cells/well from passages 3 and 12, respectively. Osteogenic differentiation was induced by seeding the cells in the osteogenic medium consisted of DMEM, supplemented with 10% FBS, 50 μg/ml ascorbate-2-phosphate, 100 nM dexamethasone (Sigma) and 10 mM β-glycerol phosphate (Sigma) for a period of 4 weeks. Osteogenesis was examined by staining for calcium deposition with alizarin red S. Cells were fixed with 70% (v/v) ethanol for 10 min at room temperature, washed 3 times with PBS, and then incubated with 0.1% (w/v) alizarin red S solution. For adipogenesis, the cells were cultured in an adipogenic medium for 3 weeks. Adipogenic medium was composed of DMEM, supplemented with 10% FBS, 50 μg/ml ascorbate-2-phosphate, 100 nM dexamethasone (Sigma), and 50 μg/ml indomethacin (Sigma). In order to assess adipogenesis, cells were stained for intracellular lipid droplets with oil red O. Cells were fixed with 10% (v/v) formalin for 30 min, washed with PBS, and incubated with 0.5% (w/v) oil red O (Sigma) for 20 min.

2.2 Preparation of injectable CH-β-GP-HEC scaffold

In this study, 150 mg chitosan (CH) powder (Polysciences, Cat. No. 21161) with a molecular weight (Mw) of 1.5×10^4 kDa was dissolved in 9 ml hydrochloric acid (80 mM) with shaking. This solution was autoclaved and cooled to 4 °C. A 10X GP (1.5 M) was prepared by dissolving 3.25 g of β-glycerol phosphate (β-GP) (Sigma, Cat. No. G-9422) in 10 ml deionized water and it was sterilized using a 0.2 μm filter. Both solutions were chilled on ice for 15 min in order to inhibit gelation. The ice-cold sterile aqueous solution of disodium-β-GP was then added to the ice-cold chitosan solution while stirring to form a clear solution. Then, prior to injecting, 0.125 g of hydroxyethyl cellulose (HEC) (Sigma-Aldrich, Cat. No. 09368) was added to the solution. The final percentages of CH:β-GF:HEC in the final solution were 1.5%:15%:0.18% (w/v), respectively [30].

2.2.1 Cell encapsulation in the CH-β-GP-HEC scaffold

8×10^6 labeled cells were suspended in 400 μl medium and then added in a dropwise manner to 7.6 ml of the prepared and chilled CH-β-GP-HEC, with continuous stirring to form a homogeneous cellular suspension.

2.3 Animal studies and xenotransplantation of hAd-MSCs

Male Wistar rats (2 months old) with an average weight of 250 g were used in this study. Animals were kept in the normal 12 h day–night cycle, at 25 ± 2 °C and 50% humidity, and fed by lab chow and tap water. All experiments were conducted in accordance with the guidelines of the Animal Care section at the Ferdowsi University of Mashhad, approved by the University Animal Ethics Committee. Eighty Wistar rats were divided into 16 groups (n = 5 in each group): sham groups (DMEM/ DMEM-Scaffold) and test groups (hAd-MSCs/ hAd-MSCs-Scaffold) and investigated at different time intervals (15, 45, 90 and 180 days). Animals in all groups were anesthetized by intraperitoneal injection of a mixture of ketamine (30 mg/kg) and xylazine hydrochloride (4 mg/kg). In test groups, cells were transplanted in the presence and/or absence of scaffold into the right upper lobe of the liver by laparotomy. To do so, rats in both sham and test groups were anesthetized and abdominal hairs were removed under aseptic conditions. Then, the right upper lobe of the liver was exposed and 2×10^5 cells suspended in 100 μl DMEM or cell-laden chitosan scaffolds were injected using a 30-gauge insulin syringe. The incision was then closed with the catgut suture. Rats in the sham groups, which were divided into scaffold-dependent and scaffold-independent, were injected with scaffold and DMEM, respectively. Finally, rats in all groups were injected intramuscularly with 5000 units of penicillin/kg body weight to avoid possible infections. All rats were kept in separate cages to recover.

2.4 Histological observation and quantification of the transplanted cells

All groups of rats were re-anesthetized as mentioned above, and sacrificed by cardiac perfusion at 15, 45, 90, and 180 days after transplantation. Their left ventricle was cannulated, and an incision was made in their right atrium, perfused with 4% (w/v) paraformaldehyde in PBS (pH 7.4) until the outflow became clear. The liver was incised in the middle and immediately fixed in 4% paraformaldehyde for at least 24 h. The fixed tissues were then embedded in paraffin and a rotary microtome (Leitz, Austria) was used to prepare 5 μm horizontal sections of the liver. On the other hand, liver tissues were snap-frozen with liquid nitrogen below − 180 °C prior to sectioning. Tissue samples were placed in a cryomold (Tissue-Tek Cryomold, Sakura Finetek, USA Inc) half-filled with Optimal Cutting Temperature (OCT) compound (Tissue-Tek OCT, Ted Pella Inc, CA, USA). Following this, the tissue was completely submerged in OCT. Cryomold containing the tissue sample in OCT was kept in the cryostat (RMC, CRT 900, Boeckeler Instruments Inc, AZ, USA) at −20 °C and left for 180 s until the OCT compound was completely frozen. Then, the frozen tissue block was removed from the cryomold and loaded onto the specimen holder. In order to obtain better sections, the temperature of both the blade stage and the specimen holder was optimized in the cryostat chamber. The sections were cut with the cryostat to access the target region and then series of the tissue sample sections were prepared with 8–10 μm tickness. Finally, the sections were kept in a desiccator with a vacuum pump in a cold room overnight. Slides were examined under a fluorescent microscope (Olympus AH3-RFCA, Japan) after staining with DAPI nucleic acid stain. In order to quantify the number of the implanted cells, as an indicator of their survival rate in the organ, ImageJ software was used. All labeled cells were monitored in 10 microscopic slides from each test, and five tests were examined each time.

2.5 DNA extraction and PCR analysis

Genomic DNA (gDNA) was extracted from various organs including spleen, liver, lung, muscle, brain, eye and testis using AccuPrep Genomic DNA Extraction Kit (BIONEER). The extracted gDNAs were subjected to polymerase chain reaction (PCR) analysis using a primer set (Macrogen, Korea) for amplification of *GFP* (220 bp PCR product). The sequences for forward and reverse primers were (5′-GATG AAGAGCACCAAAGGC-3′ and 5′-GTAGCTGAAGCTCA CGTGC-3′), respectively. The thermal cycling condition was initiated at 94 °C × 5 min for one cycle followed by 40 cycles of 94 °C × 30 s, 59 °C × 30 s, 72 °C × 30 s; and 72 °C × 10 min for final extension. At the same time, samples from the control rats were used as negative references and gDNAs from the transgenic hAd-MSCs as positive controls.

2.5.1 Quantitative real-time PCR analysis

To evaluate cell migration from the injected site, quantitative real-time PCR, for the GFP reporter gene present in the transduced cells, was performed on genomic DNAs extracted from spleens. Real-time PCR was performed using the Bio-Rad CFX-96 thermocycler. In order to generate a standard curve for absolute quantification of the spleen DNA derived from rats transplanted with cell-laden scaffolds and scaffold-free groups, serial dilutions of pLEX-JRed/TurboGFP, ranging from 8.5×10^8 to 8.5×10^2 copies μl^{-1}, were used. The concentration of the GFP encoding vector, pLEX-JRed/TurboGFP, was measured using a NanoDrop (Thermo Scientific NanoDrop 2000c), and converted to the copy concentration using the following formula: DNA (copy) = 6.02×10^{23} (copies mol^{-1}) / DNA length (bp) × 660 (g mol^{-1} bp^{-1}). Each standard dilution was processed in duplicate for further analysis. The threshold cycle (Ct) values were plotted against the logarithm of their initial template copy concentrations. Each standard curve has resulted from the linear regression of the plotted points. PCR amplification efficiency from the slope of each curve (E) was measured according to the following equation: $E = 10^{-1/\text{slope}} - 1$. All real-time PCR reactions were performed in triplicate, and each reaction mixture was prepared using the SYBR Green PCR Master Mix (Applied Biosystems) in a total volume of 20 μl:10 μl master mix, 3 μl of each gDNA sample (1 ng/μl), 0.5 μl of each primer (10 pmol/μl), and 6 μl DNase-free water. The thermal cycling conditions were as follows: initial denaturation for 5 min at 95 °C followed by 40 cycles at 95 °C for 40 s, 59 °C for 30 s, and 72 °C for 30 s.

2.6 Statistical analysis

The results are presented as mean ± standard deviation. One-way analysis of variance (ANOVA) was used to analyze the survival and migration of the injected hAd-MSCs over time. Analysis of variance was done by a Tukey post-hoc test. Statistical significance was considered at $P < 0.05$. All statistical analyses were carried out in triplicate with SPSS 16.0 (SPSS Inc., Chicago, IL, USA).

3 Results

3.1 Characterization of hAd-MSCs transduced with dual fluorescent reporters

Human Ad-MSCs were successfully extracted from liposuction waste tissues, cultured and characterized. These cells were subjected to gene manipulation for ectopic expression of reporter genes via transduction with pseudo-lentiviruses encoding TurboGFP and JRed proteins (Fig. 1A and B). On the other hand, osteogenic and adipogenic features of hAd-MSCs, before and after transduction, were confirmed by the

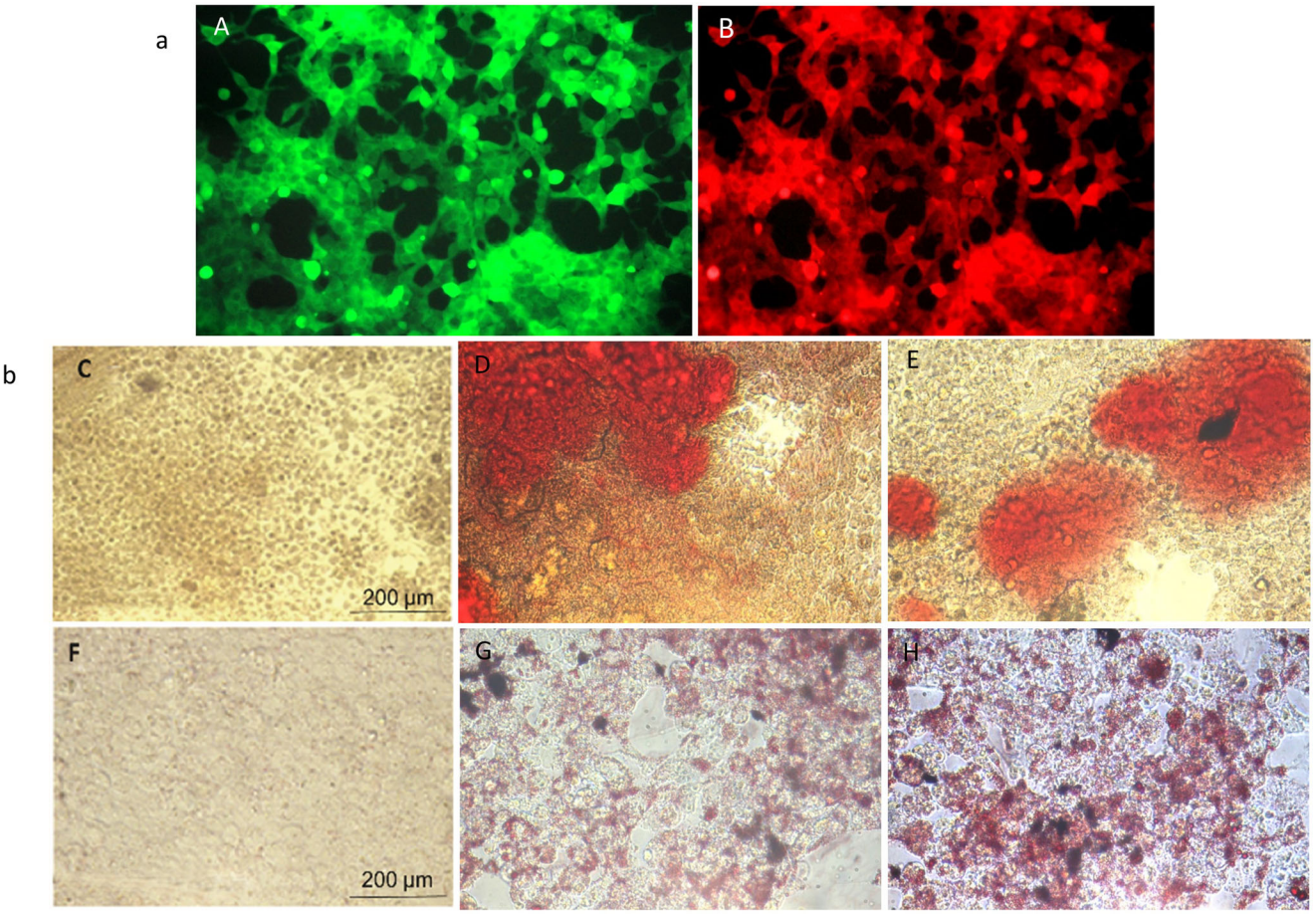

Fig. 1 a) Fluorescent microscopic images of labeled human adipose-derived mesenchymal stem cells expressing TurboGFP (A) and JRed (B) fluorescent proteins 15 days after transduction with lentiviral particles carrying the marker genes, under selection medium. b) Differentiation ability of the isolated and transduced human adipose-derived mesenchymal stem cells towards osteogenic (upper panel) and adipogenic (lower panel) lineages. C and F) the undifferentiated cells stained with alizarin red S and oil red O, D and G) differentiated cells before the viral transduction, E and H) differentiated cells after the viral transduction

appearance of the calcium deposits and lipid vacuoles, respectively (Fig. 1C–H), 3 weeks after lineage induction. Cells were also subjected to flow cytometry analysis for expression of the MSC markers, and shown to be positive for CD44, CD105, and CD90, and negative for CD34 and CD45 markers (data not shown).

3.2 Evaluating the behavior of hAd-MSCs transplanted into the rat liver

Fluorescent microscopic observation, 15 days after transplantation, indicated a great number of labeled cells at the site of injection in the right upper lobe of the liver (Fig. 2A–C). However, tracing these cells at 45, 90, and 180 days after injection demonstrated their migratory behavior into other organs, which was evidenced by a reduction in the abundance of labeled cells by time (data not shown). Moreover, the labeled cells were detectable in other parts of the liver, in particular at the lower right lobe of the liver as indicated at 15 days after transplantation (Fig. 2D–F).

3.3 Tracing transplanted hAd-MSCs encapsulated in the scaffold over a period of 6 months

In order to assess the restrictive effects of CH-β-GP-HEC scaffold on the behavior of hAd-MSCs after implantation, fluorescent microscopic observation was carried out. Fifteen days after implantation, as shown in Fig. 3A–C, network-like structures, harboring labeled cells at the right upper lobe of the liver, were developed. This indicates the restrictive features of the scaffold in confinement of the hAd-MSCs from migration. Although these structures were not detectable after this time until the end of the tracking period, i.e., 180 days after implantation, we detected the implanted cells at the right upper lobe of the liver, in both sporadic (Fig. 3D–F, 45 days after implantation) and cluster manners.

3.4 Human Ad-MSC migration to non-targeted organs after injection into the liver

To have a precise estimation for the presence of hAd-MSCs in non-targeted organs, including spleen, muscle, brain, eyes,

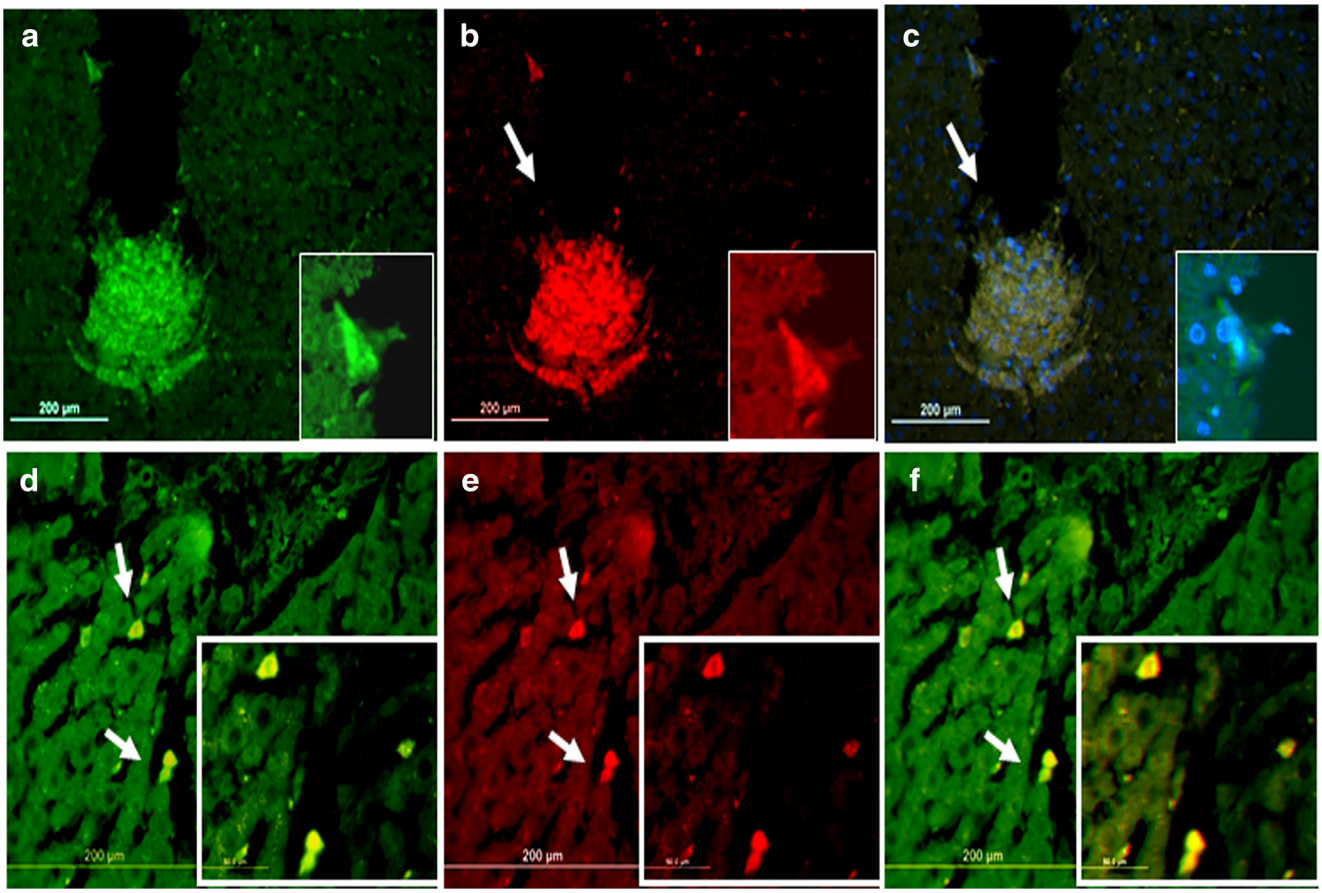

Fig. 2 a) The abundance of labeled human adipose-derived mesenchymal stem cells at the transplantation site in the right upper lobe of the liver, 15 days after transplantation. A: fluorescent microscopic image of the right upper lobe of the liver sections representing transplanted cells expressing green fluorescent protein (GFP), B: represents transplanted cells expressing JRed fluorescent protein, C: represents the merged image of DAPI stained cells expressing GFP and JRed. b) Micrographs indicating hAd-MSCs at the lower right lobe of the liver at 15 days after transplantation into the upper lobe. Migratory hAd-MSCs are indicated with arrows; D and E: represent transplanted cells expressing GFP and JRed fluorescent proteins, respectively. F: represents a merged image from D and E

lung, and testis, and evaluate the ability of scaffold in confining the cells within the injected site boundary, PCR of the *GFP* marker gene, specific to the exogenously injected cells, was employed. This analysis proved positive in gDNA samples extracted from spleen in both groups, with or without a scaffold, over a period of 6 months after injection (Fig. 4). Nonetheless, PCR analysis on the GFP marker gene from gDNA extracted from the lower lobe of the liver, lung, brain, eyes, muscle, and testis, among non-target organs, confirmed hAd-MSC migratory behavior happened only in the scaffold-free groups (Fig. 4b, A).

3.5 Quantitative assessment of the transplanted hAd-MSCs migrated into the spleen during the 6-month period

In order to compare the capacity of the CH-β-GP-HEC scaffold to prevent cell migration, the copy number of the GFP marker gene, as an indicator of the quantitative number of the labeled cells, was assessed in the spleens of both groups, which had received the labeled cells in their liver, with or without a scaffold, by qPCR. As shown in Fig. 4c, at different time intervals, the labeled cells were traced in the spleens of the two groups; however, their number was significantly lower in the spleens of the scaffold-dependent group compared to the other group, especially at 90 days after transplantation. Notably, cells revealed a decline in the *GFP* copy number on day 180 in which cells might have migrated to other tissues, or have undergone apoptosis.

4 Discussion

Mesenchymal stem cells have revealed to be a prominent resource for cell-based therapy. In particular, adipose tissues are recognized as a rich source of MSCs from which, cells can easily be harvested [14]. Human Ad-MSCs are multipotent cells with the ability to differentiate into all mesodermal lineages including chondrocytes, osteoblasts, and adipocytes. Moreover, their hepatogenic capability has been also shown

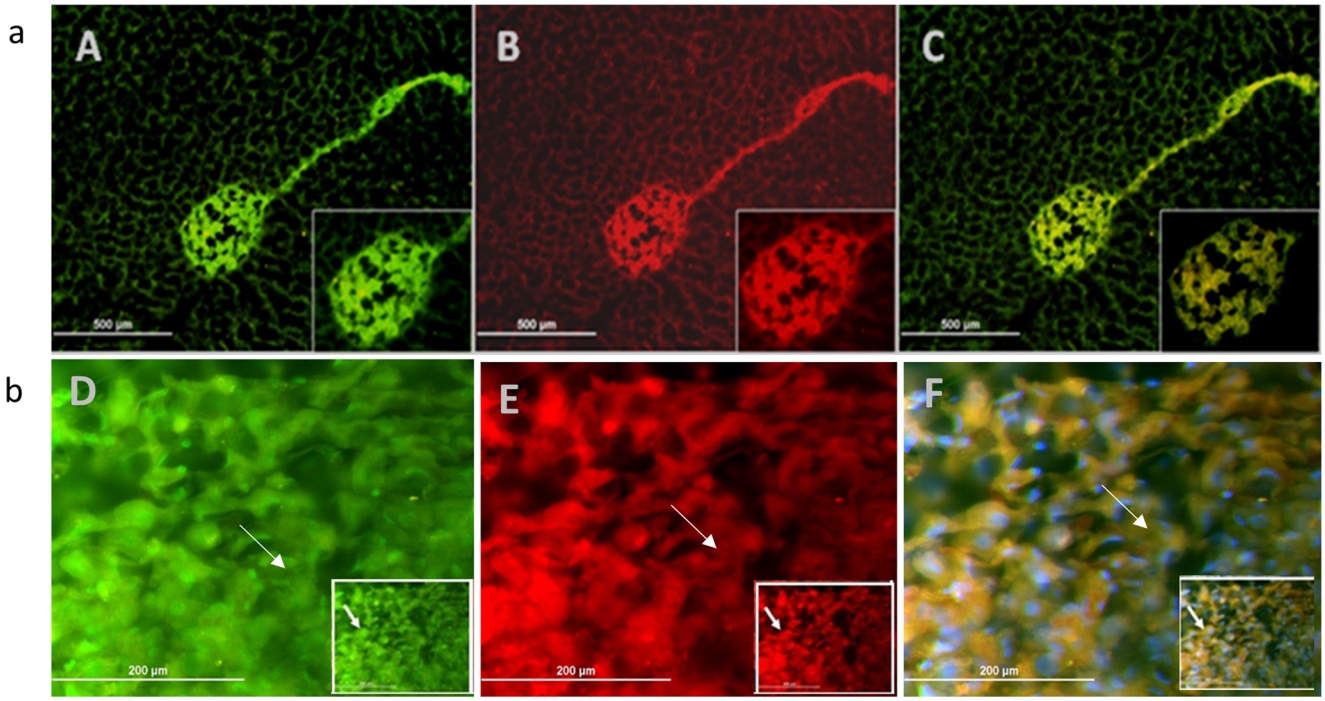

Fig. 3 a) Fluorescence microscopic images of a cryosection of the right upper lobe of the liver at 15 days after implantation of labeled human adipose-derived mesenchymal stem cells encapsulated in the scaffold. A: represents implanted cells expressing green fluorescent protein (GFP), B: represents implanted cells expressing JRed fluorescent protein, C: represents the merged image from A and B. b) Fluorescent microscopic images of the right upper lobe of the liver sections at 45 days after hAd-MSC implantation. D and E: represent implanted cells expressing GFP, and JRed, respectively. F: represents DAPI stained cells merged with the other two images from D and E. Position of cells in all images is shown with arrows

both in vitro and in vivo [31]. Different strategies have been used for transplantation of hAd-MSCs into the liver for clinical purposes. In this study, we tested the possibility of transplanting hAd-MSCs, encapsulated in a thermosensitive chitosan-based scaffold, CH-β-GP-HEC, into the adult rat liver. Our previous data revealed that this scaffold is biocompatible as it could penetrate into the liver tissue without causing considerable morphological changes. In addition, the chitosan-based scaffold showed no obvious inflammatory response for up to 6 months after transplantation [32]. In the current study, the potency of the scaffold for maintaining the transplanted cells in the liver was evaluated. A number of studies have been carried out on different natural polymers as scaffolds or carriers for MSCs in vitro and in vivo, such as alginate [33], hyaluronic acid [34] and chitosan [35]. Moreover, hydrogels are considered as cell-friendly materials, which support cellular attachment [36]. In this regard, Chen et al., created an alginate microsphere as a carrier for injection of hAd-MSCs in a hepatectomized mouse model. They detected viable MSCs around the degraded alginate microspheres in the liver and other organs such as bone marrow and lungs [17]. Jain et al., summarized the results of the majority of polymers which have been used for liver tissue engineering, although the performance of these natural polymers has not been investigated in the liver tissue, directly [37]. Similarly, Xu et al. fabricated a silk fibroin construct seeded by MSCs for liver regeneration. MSCs-seeded in the silk fibroin scaffold exhibited excellent biocompatibility and hepatogenic differentiation in vitro. Furthermore, the function of cells seeded in the scaffold was improved when it was implanted into mice liver, which resulted in angiogenesis and differentiation [38]. Due to the excellent properties including biodegradability, biocompatibility, and cellular attachment, hydrogels are considered a suitable scaffold for tissue engineering among other natural polymers [39]. We also showed that the thermosensitive chitosan-based scaffold, CH-β-GP-HEC, was biodegradable upon implantation into the adult rat liver [32]. In this study, we further aimed to investigate the CH-β-GP-HEC contribution to confinement of the transplanted hAd-MSCs in the rat liver, using GFP and JRed as tracking markers. GFP has been considered a nontoxic and safe marker with high sensitivity and specificity in cells analyzed by flow cytometry in living, fixed, and frozen cells [40]. For this purpose, we developed a vector, expressing both GFP and JRed as reporters to track the fate of the implanted cells. The transduced cells successfully expressed the reporter proteins as shown in Fig. 1, indicating their full integration into the host genome. As for their characterization, the transduced cells behaved similar to control cells in response to differentiation conditions (Fig. 1) and also expressed similar cell surface markers. In order to investigate if the prepared chitosan-based scaffold could support the engraftment of

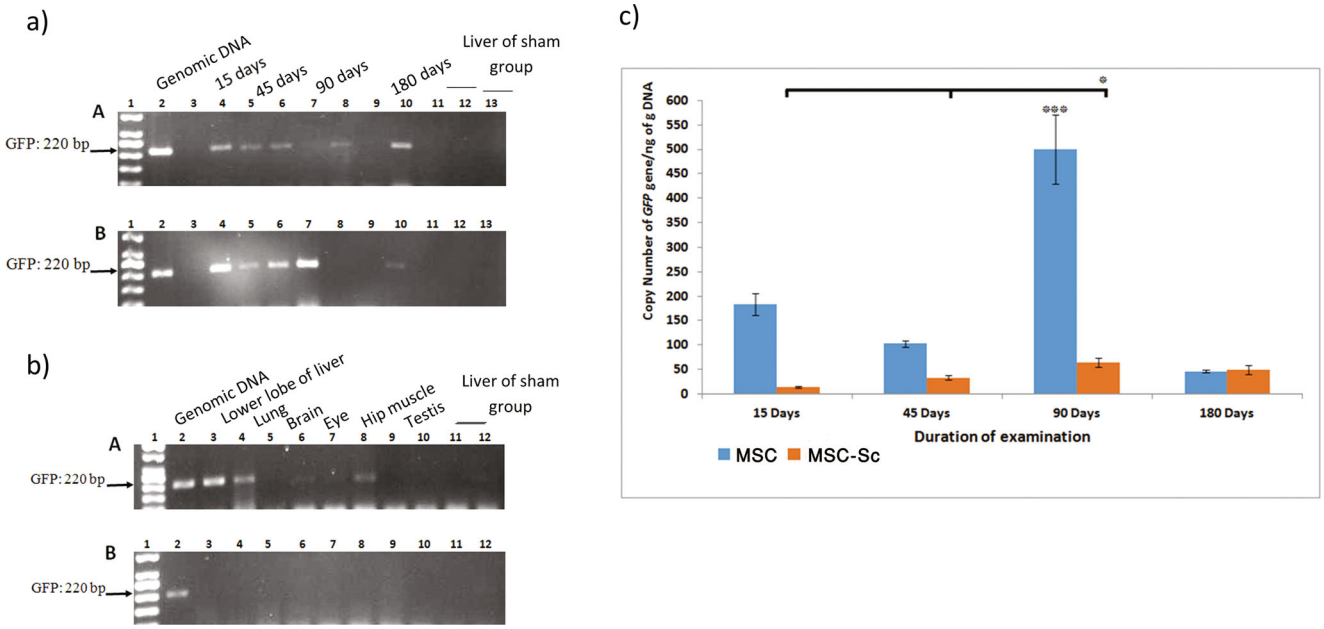

Fig. 4 a) Assessing the migratory behavior of hAd-MSCs after injection to the rat liver without (A) and with (B) scaffold, during 6-month follow-up, based on PCR products for GFP encoding gene. The lanes represent 1) 50 bp DNA ladder, 2) gDNA PCR product, as a positive control, from the cultured transduced hAd-MSCs in vitro, 3–11) PCR products on gDNAs extracted from spleens of different rats in the test group during 6 months post-injection, including lanes 3 and 4 (15 days), lanes 5 and 6 (45 days), lanes 7 and 8 (90 days), and lanes 9, 10 and 11 (180 days). Lanes 12 and 13 correspond to PCR on the spleen DNA of non-transplanted rats as a negative control and transplanted rats with PBS as vehicle control, respectively. Lane 13 in lower panel corresponds to PCR on spleen DNA of rats implanted with PBS + scaffold as vehicle control. b) GFP PCR products, as a specific marker in the hAd-MSCs, confirm the migratory behavior of transplanted cells from the liver to non-target organs (panel A), as well as the capability of the scaffold to prevent migration (panel B) at 90 days after injection. The lanes represent 1) 50 bp DNA ladder, 2) PCR product on gDNA, as a positive control, from the cultured transduced hAd-MSCs, 3–10) PCR products on gDNAs extracted from non-target tissues and organs including lower lobe of the liver (lane 3), lung (lane 4), brain (lanes 5 and 6), eyes (lane 7), hip muscle (lane 8), and testis (lanes 9 and 10) at 90 days after injection. Lanes 11 and 12 correspond to PCR products on the spleen DNA of negative control and vehicle control, respectively. c) The copy number of GFP as an indicator of hAd-MSCs accumulated in rat spleens during 6 months after transplantation to the liver with (MSC-Sc) or without a scaffold (MSC), as examined by absolute real-time PCR based on *GFP* gene (***$P \leq 0.001$, *$P \leq 0.05$). All error bars indicate the standard deviation (SD)

labeled cells in the liver, xenotransplantation was performed. A considerable number of GFP and JRed positive cells transplanted in the upper right lobe of the liver in the scaffold-free group were seen at 15 days post-transplantation, while, the fluorescent signal gradually decreased over time. A probable reason for this observation is the migration of cells from the upper part of the liver to the lower part (Fig. 2). Further experiments were performed with cells encapsulated in the scaffold and transplanted into the rat liver. Our study indicated that a high number of cells accumulated in the upper right lobe as a sign of the presence of the scaffold at day 15 after implantation (Fig. 3). Although GFP and JRed expressing cells could be traced for 180 days after transplantation, the fluorescence tended to die gradually. We examined cell migration into other main organs including spleen, lung, brain, eyes, muscle, and testis. The results indicated that the labeled cells from the scaffold group could spread into the spleen. However, cells in the scaffold-free group showed a broader migration to other mentioned organs (Fig. 4). Quantitative amplification of *GFP* showed (Fig. 4c) its higher copy number in the spleens of scaffold-free groups compared to those delivered via the scaffold at days 15 and 90 and dropped on day 180 post-transplantation. While the *GFP* copy number dropped significantly at day 180, the GFP labeled cells could still be traced until this time in the spleen. The current study suggests that the exogenous hAd-MSCs could survive in the rat liver in both groups. Particularly, cells encapsulated in the thermosensitive chitosan-based scaffold displayed less migration to other organs, thereby opening the possibility to use this strategy for therapeutic purposes. Further studies are required to investigate the behavior of the cells after transplantation, their migration, and in situ differentiation in particular.

5 Conclusion

Our results showed that labeled cells encapsulated in the chitosan-glycerol phosphate hydrogel can be well retained in the rat liver for at least 180 days in comparison to scaffold-free cell implantation. Therefore, such combination could serve as an efficient way for delivery and maintenance of the cells in the liver for therapeutic purposes, as including the scaffolds in combination with cells could prevent their migration to other

tissues. This strategy might be efficient for therapeutic applications in other organs and for a gradual release of desired molecules like drugs; however, further studies are required to confirm this.

Acknowledgements The authors thank Ehsan Bahramzadeh and Mohammadmahdi Esmail-Jami for their editing suggestions, as well as Hassan Tamadonipour, Mohammad Nakhaei, and Dr. Moein Farschian for their excellent technical assistance.

Author contribution AHM, MMM, and ARB were responsible for the design of experiments and data acquisition, and data interpretation; FS, SE, and AZ contributed to data analysis and manuscript preparation. All authors approved the final version of the manuscript.

Funding The study was financed by grants from Ferdowsi University of Mashhad and Iran National Science Foundation (INSF) and performed in the Institute of Biotechnology, Ferdowsi University of Mashhad.

Declarations

Ethics approval and consent to participate The authors declare that the research was conducted with the approval from Ferdowsi University of Mashhad Ethics Committee (IR.UM.REC.1399.069). Written informed consents were obtained from the patients.

Conflict of interest The authors declare no competing interests.

References

1. P. Marcellin, B.K. Kutala, *Liver diseases: A major, neglected global public health problem requiring urgent actions and large-scale screening*. Liver Int. **38**, 2–6 (2018)
2. C. Hu, Z. Wu, L. Li, *Pre-treatments enhance the therapeutic effects of mesenchymal stem cells in liver diseases*. J. Cell. Mol. Med. **24**(1), 40–49 (2020)
3. A. Sun, W. Gao, T. Xiao, *Autologous bone marrow stem cell transplantation via the hepatic artery for the treatment of hepatitis B virus-related cirrhosis: A PRISMA-compliant meta-analysis based on the Chinese population*. Stem Cell Res Ther **11**(1), 1–17 (2020)
4. V. Iansante, R.R. Mitry, C. Filippi, E. Fitzpatrick, A. Dhawan, *Human hepatocyte transplantation for liver disease: Current status and future perspectives*. Pediatr. Res. **83**(1), 232–240 (2018)
5. L.J. Wang, Y.M. Chen, D. George, F. Smets, E.M. Sokal, E.G. Bremer, H.E. Soriano, *Engraftment assessment in human and mouse liver tissue after sex-mismatched liver cell transplantation by real-time quantitative PCR for Y chromosome sequences*. Liver Transpl. **8**(9), 822–828 (2002)
6. C. Hu, L. Li, *In vitro culture of isolated primary hepatocytes and stem cell-derived hepatocyte-like cells for liver regeneration*. Protein Cell **6**(8), 562–574 (2015)
7. M.F. Pittenger et al., *Multilineage potential of adult human mesenchymal stem cells*. Science **284**(5411), 143–147 (1999)
8. K. Bieback, S. Kern, H. Klüter, H. Eichler, *Critical parameters for the isolation of mesenchymal stem cells from umbilical cord blood*. Stem Cells **22**(4), 625–634 (2004)
9. S.A. Scherjon et al., *Isolation of mesenchymal stem cells of fetal or maternal origin from human placenta*. Stem Cells **22**(7), 1338–1345 (2004)
10. D.T.b. Shih et al., *Isolation and characterization of neurogenic mesenchymal stem cells in human scalp tissue*. Stem Cells **23**(7), 1012–1020 (2005)
11. P. De Coppi et al., *Isolation of amniotic stem cell lines with potential for therapy*. Nat. Biotechnol. **25**(1), 100–106 (2007)
12. P.A. Zuk, M. Zhu, H. Mizuno, J. Huang, J.W. Futrell, A.J. Katz, P. Benhaim, H.P. Lorenz, M.H. Hedrick, *Multilineage cells from human adipose tissue: Implications for cell-based therapies*. Tissue Eng. **7**(2), 211–228 (2001)
13. K. Furuhashi, N. Tsuboi, A. Shimizu, T. Katsuno, H. Kim, Y. Saka, T. Ozaki, Y. Sado, E. Imai, S. Matsuo, S. Maruyama, *Serum-starved adipose-derived stromal cells ameliorate crescentic GN by promoting immunoregulatory macrophages*. J. Am. Soc. Nephrol. **24**(4), 587–603 (2013)
14. Y. Fu, J. Deng, Q. Jiang, Y. Wang, Y. Zhang, Y. Yao, F. Cheng, X. Chen, F. Xu, M. Huang, Y. Yang, S. Zhang, D. Yu, R.C. Zhao, Y. Wei, H. Deng, *Rapid generation of functional hepatocyte-like cells from human adipose-derived stem cells*. Stem Cell Res Ther **7**(1), 105 (2016)
15. H. Okura, M. Soeda, M. Morita, M. Fujita, K. Naba, C. Ito, A. Ichinose, A. Matsuyama, *Therapeutic potential of human adipose tissue-derived multi-lineage progenitor cells in liver fibrosis*. Biochem. Biophys. Res. Commun. **456**(4), 860–865 (2015)
16. N. Liao et al., *Poly (dopamine) coated superparamagnetic iron oxide nanocluster for noninvasive labeling, tracking, and targeted delivery of adipose tissue-derived stem cells*. Sci. Rep. **6**, 18746 (2016)
17. M.-J. Chen, Y. Lu, N.E. Simpson, M.J. Beveridge, A.S. Elshikha, M.A. Akbar, H.Y. Tsai, S. Hinske, J. Qin, C.R. Grunwitz, T. Chen, M.L. Brantly, S. Song, *In situ transplantation of alginate bioencapsulated adipose tissues derived stem cells (ADSCs) via hepatic injection in a mouse model*. PLoS One **10**(9), e0138184 (2015)
18. H. Li, B. Zhang, Y. Lu, M. Jorgensen, B. Petersen, S. Song, *Adipose tissue-derived mesenchymal stem cell-based liver gene delivery*. J. Hepatol. **54**(5), 930–938 (2011)
19. M. Saheli et al., *Generation of transplantable three-dimensional hepatic-patch to improve the functionality of hepatic cells in vitro and in vivo*. Stem Cells Dev. **29**(5), 301–313 (2020)
20. C. Siltanen, M. Diakatou, J. Lowen, A. Haque, A. Rahimian, G. Stybayeva, A. Revzin, *One step fabrication of hydrogel microcapsules with hollow core for assembly and cultivation of hepatocyte spheroids*. Acta Biomater. **50**, 428–436 (2017)
21. N. Mobarra, M. Soleimani, F. Kouhkan, Z. Hesari, R. Lahmy, M. Mossahebi-Mohammadi, E. Arefian, Z. Jaafarpour, H. Nasiri, R. Pakzad, R. Tavakoli, P. Pasalar, *Efficient differentiation of human induced pluripotent stem cell (hiPSC) derived hepatocyte-like cells on hMSCs feeder*. Int. J. Hematol.-Oncol Stem Cell Res. **8**(4), 20–29 (2014)
22. M. Saheli, M. Sepantafar, B. Pournasr, Z. Farzaneh, M. Vosough, A. Piryaei, H. Baharvand, *Three-dimensional liver-derived extracellular matrix hydrogel promotes liver organoids function*. J. Cell. Biochem. **119**(6), 4320–4333 (2018)
23. J.F. Prudden, P. Migel, P. Hanson, L. Friedrich, L. Balassa, *The discovery of a potent pure chemical wound-healing accelerator*. Am. J. Surg. **119**(5), 560–564 (1970)
24. R. Muzzarelli, V. Baldassarre, F. Conti, P. Ferrara, G. Biagini, G. Gazzanelli, V. Vasi, *Biological activity of chitosan: Ultrastructural study*. Biomaterials **9**(3), 247–252 (1988)
25. P.J. VandeVord, H.W.T. Matthew, S.P. DeSilva, L. Mayton, B. Wu, P.H. Wooley, *Evaluation of the biocompatibility of a chitosan scaffold in mice*. J. Biomed. Mater. Res. **59**(3), 585–590 (2002)
26. C. Hoemann et al., *Cytocompatible gel formation of chitosan-glycerol phosphate solutions supplemented with hydroxyl ethyl cellulose is due to the presence of glyoxal*. J. Biomed. Mater. Res. A **83**(2), 521–529 (2007)

27. A. Chenite, C. Chaput, D. Wang, C. Combes, M.D. Buschmann, C.D. Hoemann, J.C. Leroux, B.L. Atkinson, F. Binette, A. Selmani, *Novel injectable neutral solutions of chitosan form biodegradable gels in situ*. Biomaterials **21**(21), 2155–2161 (2000)
28. C. Hoemann et al., *Tissue engineering of cartilage using an injectable and adhesive chitosan-based cell-delivery vehicle*. Osteoarthr. Cartil. **13**(4), 318–329 (2005)
29. J. Gimble, F. Guilak, *Adipose-derived adult stem cells: Isolation, characterization, and differentiation potential*. Cytotherapy **5**(5), 362–369 (2003)
30. H. Naderi-Meshkin, K. Andreas, M.M. Matin, M. Sittinger, H.R. Bidkhori, N. Ahmadiankia, A.R. Bahrami, J. Ringe, *Chitosan-based injectable hydrogel as a promising in situ forming scaffold for cartilage tissue engineering*. Cell Biol. Int. **38**(1), 72–84 (2014)
31. A. Seki, Y. Sakai, T. Komura, A. Nasti, K. Yoshida, M. Higashimoto, M. Honda, S. Usui, M. Takamura, T. Takamura, T. Ochiya, K. Furuichi, T. Wada, S. Kaneko, *Adipose tissue-derived stem cells as a regenerative therapy for a mouse steatohepatitis-induced cirrhosis model*. Hepatology **58**(3), 1133–1142 (2013)
32. A. Haddad-Mashadrizeh et al., *Cytotoxicity and biocompatibility evaluation of chitosan-beta glycerol phosphate-hydroxyethyl cellulose hydrogel on adult rat liver for cell-based therapeutic applications*. Int. J. Biomed. Eng. Technol. **12**(3), 228–239 (2013)
33. A. Pirosa, R. Gottardi, P.G. Alexander, R.S. Tuan, *Engineering in-vitro stem cell-based vascularized bone models for drug screening and predictive toxicology*. Stem Cell Res Ther **9**(1), 112 (2018)
34. M. Kim, I.E. Erickson, A.H. Huang, S.T. Garrity, R.L. Mauck, D.R. Steinberg, *Donor variation and optimization of human mesenchymal stem cell chondrogenesis in hyaluronic acid*. Tissue Eng. A **24**(21-22), 1693–1703 (2018)
35. T. Liu, J. Li, Z. Shao, K. Ma, Z. Zhang, B. Wang, Y. Zhang, *Encapsulation of mesenchymal stem cells in chitosan/β-glycerophosphate hydrogel for seeding on a novel calcium phosphate cement scaffold*. Med. Eng. Phys. **56**, 9–15 (2018)
36. F. Shahabipour, N. Ashammakhi, R.K. Oskuee, S. Bonakdar, T. Hoffman, M.A. Shokrgozar, A. Khademhosseini, *Key components of engineering vascularized 3-dimensional bioprinted bone constructs*. Transl. Res. **216**, 57–76 (2020)
37. E. Jain, A. Damania, A. Kumar, *Biomaterials for liver tissue engineering*. Hepatol. Int. **8**(2), 185–197 (2014)
38. L. Xu, S. Wang, X. Sui, Y. Wang, Y. Su, L. Huang, Y. Zhang, Z. Chen, Q. Chen, H. du, Y. Zhang, L. Yan, *Mesenchymal stem cell-seeded regenerated silk fibroin complex matrices for liver regeneration in an animal model of acute liver failure*. ACS Appl. Mater. Interfaces **9**(17), 14716–14723 (2017)
39. H. Naderi, M.M. Matin, A.R. Bahrami, *Review paper: critical issues in tissue engineering: biomaterials, cell sources, angiogenesis, and drug delivery systems*. J. Biomater. Appl. **26**(4), 383–417 (2011)
40. M.A. Rizzo, M.W. Davidson, D.W. Piston, *Fluorescent protein tracking and detection: Fluorescent protein structure and color variants*. Cold Spring Harb Protoc **2009**(12), pdb. top63 (2009)